A Study on the Frequency Response Characteristics of High Response Flow Control Servo Valve

Jong Soo Seo, You Sik Shin, Young Heung Chun*, Hyo Min Jeong*, Han Shik Chung*†
Graduate School of Precision Mechanical Engineering, Gyeongsang National Univ., Tongyeong 650-160, Korea
**School of Mechanical and Aerospace Engineering, Gyeongsang National Univ., Tongyeong 650-160, Korea*

Key words: Dynamic characteristics, Sensitivity, Amplitude ratio, Phase difference

ABSTRACT: The purpose of this research is to derive the principal design parameters governing the dynamic characteristics of the high response flow control servo valve. For this purpose, a numerical modeling of the servo valve system and a parameter sensitivity analysis to a frequency response characteristics were performed. As a result of these analysis, a basis for improvement of a dynamic characteristics of servo valve was arranged.

Nomenclature

b : feedback spring length [m]
B_f : flapper effective damping coefficient [m-N-s]
B_s : spool effective damping coefficient [N/s]
C_d : spool discharge coefficient
C_{dd} : drain orifice discharge coefficient
C_{do} : fixed orifice discharge coefficient
C_{df} : nozzle effective discharge coefficient
C_v : spool volume coefficient
D : spool diameter [m]
D_d : drain orifice diameter [m]
D_n : nozzle diameter [m]
D_o : fixed orifice diameter [m]
J_f : armature-flapper rotational inertia [m-N-s^2]
K_f : flexure tube stiffness [N/m]
K_t : torque motor gain
K_w : feedback spring stiffness [N/m]
M_s : spool mass [kg]
V_d : drain chamber volume [m^3]
V_o : contained volume at each end of spool [m^3]
X_{f0} : clearance between flapper and nozzle at null [m]
X_{mv} : spool max. displacement from null [m]

Greek symbols

ρ : hydraulic oil density [kg-s^2/m]
β : oil effective bulk modulus [m^2/N]
γ : flapper length [m]

† Corresponding author
Tel.: +82-55-640-3185; fax: +82-55-640-3188
E-mail address: hschung@nongae.gsnu.ac.kr

1. Introduction

In general, servo or servo mechanism mean an organized control system in order that the system follow random variations of target value by controlling position, velocity, acceleration, and attitude of an object. Electrohydraulic servovalve is valve for controlling oil flow or pressure of hydraulic system, which valve, in general, controls hundreds kg/cm^2 of pressure and thousands lpm of flow through weak electric signal in about some mA. Electrohydraulic servovalve is an important part that decides the whole capacity of control system, in case of configuring hydraulic servo control system of the various industrial heavy equipments, robots, aircraft, and satellite. Therefore, in behalf of competing with advanced nations in the area of up-to-date technology in the future, the most important tasks are attaining localized hydraulic servovalve skill and servo control system's design skill. Accordingly, the skill for interpreting dynamic characteristics[1] of servovalve as well as the skill for designing electric machine are surely obtained, which typically come under mechatronics technology development. In particular, electrohydraulic servovalve of a nozzle-flapper type was developed by Moog in U.S., and established theoretically by Merritt.[2] Afterwards, a study on characteristics of nozzle-flapper part's pressure and flow was done by Feng[3] who offered experimental apparatus and experimental value toward nozzle's spraying power and spraying coefficient. Lin and Akers[4,5] predicted the capacity of nozzle-flapper valve and presented their study results. This thesis analyzed modeling of the whole servovalve system and interpreted sensitivity toward frequency response characteristics in order to derive influences of each parameter on the whole system's dynamic characteristics through a quantitative (numerical) analysis.

2. Numerical analysis for servo valve

2.1 Summary of servo valve

Types of Electrohydraulic servovalve are clas- 'ied into nozzle-flapper type, z-pipe type, de- tor type, and other types according to main 'es, which sorted into 1 step, 2 step, and 3 according to amplification steps. They are livided into flow control type, pressure type, and pressure-flow control type ac- to control types, are classified into di-)ack way, position feedback way, pres- ack way according to feedback ways.

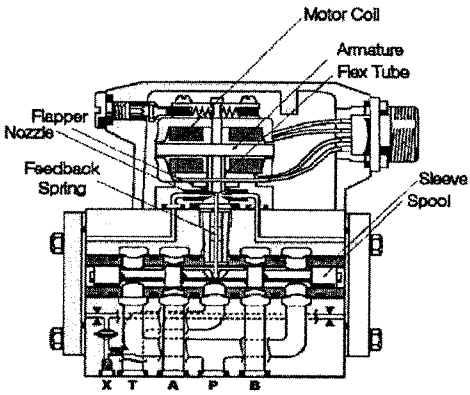

Fig. 1 Schematic diagram of a typical electro-hydraulic servo valve.

This thesis studied flow control electrohydraulic servo valve of nozzle-flapper type. which 2 step power feedback way. The basic structure is shown in Fig. 1.

2.2 Analysis for nozzle-flapper

Mathematical model of each operative torque is decided as follows;

(1) Magnetictorque

$$T_t = K_t \cdot i \tag{1}$$

(2) Torque by flexure tube

$$T_f = K_f \cdot \theta \tag{2}$$

(3) Torque by feedback spring

$$\begin{aligned} T_s &= M_s + F_s \cdot r \\ &= K_w \cdot [(r+b)\theta - x_v](r+b) \end{aligned} \tag{3}$$

(4) Torque by flow force in flapper-nozzle part

$$\begin{aligned} F_h &= (F_1 - F_2) \cdot r \\ &= (P_{n1} - P_{n2}) A_N \cdot r \\ &\quad + 4\pi C_{df}^2 [(x_{f0} + x_f)^2 (P_{n1} - P_e) \\ &\quad - (x_{f0} - x_f)^2 (P_{n2} - P_e)] \cdot r \end{aligned} \tag{4}$$

(5) Derivation of flapper movement equation

$$J_f \cdot \frac{d^2\theta}{dt^2} + B_f \cdot \frac{d\theta}{dt} = T_t + T_h - T_s - T_f \quad (5)$$

Figure 2 presents a various torque that are generated in armature-flapper assembly part when inputting electric current into torque motor.

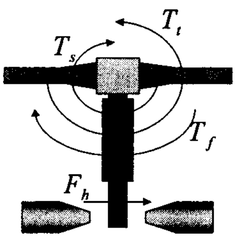

Fig. 2 Acting force on flapper-nozzle assembly.

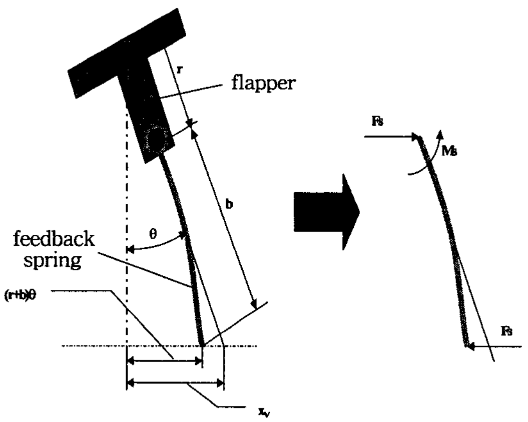

Fig. 3 Acting force on feedback spring.

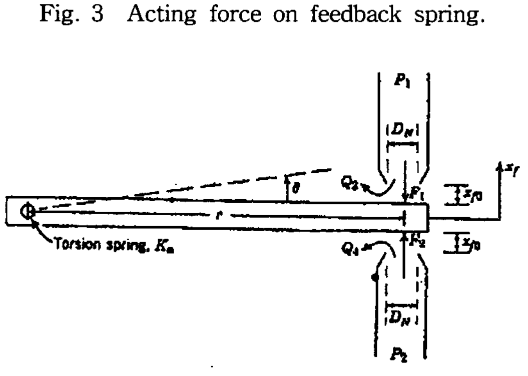

Fig. 4 Flapper-nozzle.

Figure 3 shows that there is counteraction between Fs, force given to both ends of feedback spring and moment Ms on the lower part (connecting point) of flapper.

Figure 4 represents flowing force operating flapper through fluid coming forth out of nozzle of both-side-spraying flapper valve.

2.3 Analysis for spool-sleeve

Figure 5 is a detail drawing of hydraulic servovalve's spool. Flow passing through orifice from feed line is supplied to flapper-nozzle part of valve. Force operating here on to valve spool is divided into flow force F_f and F_h, generating by pressure from spool's both ends, and F_s generating by feedback spring.

2.3.1 Continuity equation of spool inside

Pressure change shown in each chamber from hydraulic servovalve's feed line to spool's cross section, and nozzle part as well as inside of drain orifice are decided by following continuity equation.

$$\frac{dP_{n1}}{dt} = \frac{\beta}{V_1} \cdot (Q_{s1} - Q_{n1} - A_s \dot{x}_v) \quad (6)$$

$$\frac{dP_{n2}}{dt} = \frac{\beta}{V_2} \cdot (Q_{s2} - Q_{n2} + A_s \dot{x}_v) \quad (7)$$

Here,

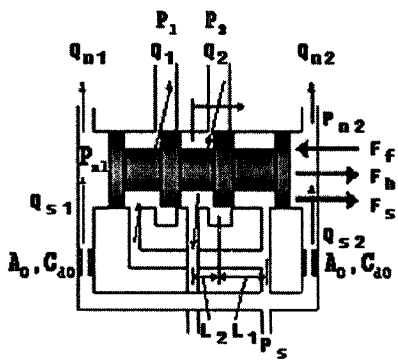

Fig. 5 Structure of spool valve.

$$V_1 = V_0 + A_s \cdot x_v,\ V_2 = V_0 - A_s \cdot x_t \qquad \frac{dP_e}{dt} = \frac{\beta}{V_d} \cdot (Q_{n1} + Q_{n2} - Q_d) \tag{8}$$

2.3.2 Movement equation of spool valve

In case that fluid accelerates or decelerates by fluid · flow change inside valve chamber, a transient state flow force equation inside each chamber is as follow;

$$\overline{F_t} = (L_1 - L_2) Cd\omega \sqrt{\rho(P_S - P_L)} \frac{\overline{dx_t}}{dt} \tag{9}$$

Normal state flow force equation that prevents valve's opening because of increasing pressure-differences caused by spraying velocity changes of fluid flowing throttle part by fluid's flowing area control is as follows;

$$\begin{aligned} \overline{F_S} &= \rho Q_1 \frac{Q_1}{C_C \cdot wx_v} \cos\theta \\ &+ \rho Q_2 \frac{Q_2}{C_C \cdot wx_v} \cos\theta \\ &= 2C_d C_v \omega (P_S - P_L) x_v \cos\theta \end{aligned} \tag{10}$$

Here, θ is jet angle. Also, flowing force operating onto valve spool is presented as follows;

$$\overline{F_f} = \overline{F_S} + \overline{F_t} \tag{11}$$

Force generating by pressure of both valve spool's ends is as follows;

$$F_h = (P_{n1} - P_{n2}) A_s \tag{12}$$

Therefore, valve spool's movement equation derived after synthesizing the above equations is shown in Eqs. 13 and 14.

$$M_s \frac{d^2 x_v}{dt^2} + B_s \frac{dx_v}{dt} = (P_{n1} - P_{n2}) A_s + F_S - F_f \tag{13}$$

$$\begin{aligned} (P_{n1} - P_{n2}) A_s + K_w (r + b)\theta &= M_s \frac{d^2 x_v}{dt^2} \\ &+ \{B_s + (L_1 - L_2) C_d \omega (P_S - P_L)\} \frac{dx_v}{dt} \\ &+ \{2C_d C_v \omega (P_S - P_L) \cos\gamma + K_w\} \cdot x_v \end{aligned} \tag{14}$$

3. Sensitivity analysis for frequency response characteristics

As for scale showing dynamic characteristics of electrohydraulic servovalve, frequency response characteristics are generally used. As for frequency response characteristics, frequency-e in which 90° phase difference is shown from the system's bode plot is defined as bandwidth of hydraulic servovalve, then, they are descried by minimum input-output ratio in this zone. And it becomes an important design specifications of the system.

3.1 Model linearization and derivation of transfer function

3.1.1 Linearization for the model of hydraulic servovalve

In order to predict hydraulic servovalve's frequency response characteristics from mathematical model, the process of model linearization is required. For this model linearization, values should be defined at hydraulic servovalve state variables' operating point. Above all, in order to identically state range of each state variables' values, normalized state variable need to be defined as shown in following equation, then, linearization model should be stated with use of it.

$$\overline{x_v} = \frac{x_v}{x_{vm}},\quad \dot{\overline{x_v}} = \frac{\dot{x_v}}{x_{vm}} \tag{15}$$

$$\overline{\theta} = \frac{\theta}{\theta_m},\quad \dot{\overline{\theta}} = \frac{\dot{\theta}}{\theta_m} \tag{16}$$

$$\overline{P}_{n1} = \frac{P_{n1}}{P_S},\quad \overline{P}_{n2} = \frac{P_{n2}}{P_S},\quad \overline{P}_e = \frac{P_e}{P_S} \tag{17}$$

Values at 7 state variables' operating points, which state the mathematical model of hydraulic servovalve are calculated as follows. First, values at operating points of spool disposition, spool velocity, flapper's rotational disposition, and flapper's rotational velocity are expressed as follows;,

$$x_v = 0,\ \dot{x}_v = 0 \tag{18}$$

$$\theta = 0,\ \dot{\theta} = 0 \tag{19}$$

Also, pressure at null of both-ends' nozzle chamber and drain chamber is derived from normal state governing equations, i.e., in case of no pressure change in each chamber, Eqs. 20 and 21 are settled;

$$(\overline{P}_{n1})_{op} = (\overline{P}_{n2})_{op} = \overline{P}_0,\ (\overline{P}_e)_{op} = \overline{P}_{e0}$$

$$C_{do}A_o\sqrt{\frac{2P_S}{\rho}}\cdot\sqrt{1-\overline{P}_0} - C_{df}D_n\pi x_{f0}\sqrt{\frac{2P_S}{\rho}}\cdot\sqrt{\overline{P}_0-\overline{P}_{e0}} = 0 \tag{20}$$

$$2C_{df}D_n\pi x_{f0}\sqrt{\frac{2P_S}{\rho}}\cdot\sqrt{\overline{P}_0-\overline{P}_{e0}} - C_{dd}A_d\sqrt{\frac{2P_S}{\rho}}\cdot\sqrt{\overline{P}_{e0}} = 0 \tag{21}$$

Normal state pressure is calculated as follows, at operating point of each chamber, through the above equation.

$$\overline{P}_0 = \frac{R_s^2(1+R_d^2)}{1+R_s^2(1+R_d^2)} \tag{22}$$

$$\overline{P}_{e0} = \frac{R_s^2R_d^2}{1+R_s^2(1+R_d^2)} \tag{23}$$

Here, R_s and R_d are expressed by Eqs. 24 and 25.

$$R_s = \frac{C_{do}A_o}{C_{df}D_n\pi x_{f0}} \tag{24}$$

$$R_d = \frac{2C_{df}D_n\pi x_{f0}}{C_{dd}A_d} \tag{25}$$

In accordance, if linearizing the non-linear differential equation by the operating point standard, which describes dynamic behavior of hydraulic servovalve, following expressions are derives;

Movement equation of flapper

$$J_a\frac{d^2\theta}{dt^2} + B_a\frac{d\theta}{dt} + K_a\theta = K_1(\Delta\overline{P}_{n1} - \Delta\overline{P}_{n2}) + K_m\overline{i} + K_2\overline{x}_v \tag{26}$$

Here,

$$J_a = J_f,\quad B_a = B_f$$

$$K_a = K_f + K_w(r+b)^2 - 16\pi C_{df}^2 x_{f0} r^2 P_S(\overline{P}_0 - \overline{P}_{e0})$$

$$K_1 = \frac{P_SA_nr}{\theta_m} + \frac{4\pi C_{df}^2x_{f0}^2rP_S}{\theta_m}$$

$$K_2 = \frac{K_w(r+b)x_{vm}}{\theta_m},\quad K_m = \frac{K_ti_{rat}}{\theta_m}$$

Movement equation of spool

$$M_v\frac{d^2x_v}{dt^2} + B_v\frac{dx_v}{dt} + K_vx_v = K_3(\Delta\overline{P}_{n1} - \Delta\overline{P}_{n2}) + K_4\overline{\theta} \tag{27}$$

Here,

$$M_v = M_s$$

$$B_v = B_s + (L_1 - L_2)C_dw\sqrt{\rho(P_S - P_L)}$$

$$K_v = K_w + 2C_dC_vw(P_S - P_L)\cos\gamma$$

$$K_3 = \frac{P_SA_s}{x_{vm}},\quad K_4 = \frac{K_w(r+b)\theta_m}{x_{vm}}$$

Differential equation for a pressure in nozzle chamber

$$\frac{d}{dt}(\Delta\overline{P}_{n1}) = -K_p\Delta\overline{P}_{n1} - K_\theta\overline{\theta} - K_l\frac{dx_v}{dt} + K_r\Delta\overline{P}_e \tag{28}$$

$$\frac{d}{dt}(\Delta\bar{P}_{n2}) = -K_p\Delta\bar{P}_{n2}+K_\theta\bar{\theta} + K_l\frac{dx_v}{dt}+K_r\Delta\bar{P}_e \tag{29}$$

Here,

$$K_p=\frac{\beta}{V_0P_S}\left\{C_{do}A_o\sqrt{\frac{2P_S}{\rho}}\cdot\left(\frac{1}{2\sqrt{1-\bar{P}_0}}\right) + C_{df}D_n\pi x_{f0}\sqrt{\frac{2P_S}{\rho}}\left(\frac{1}{2\sqrt{\bar{P}_0-\bar{P}_{e0}}}\right)\right\}$$

$$K_\theta=\frac{\beta}{V_0P_S}C_{df}D_n\pi r\theta_m\sqrt{\frac{2P_S}{\rho}}\cdot\sqrt{\bar{P}_0-\bar{P}_{e0}}$$

$$K_l=\frac{\beta A_s x_{vm}}{V_0P_S}$$

$$K_r=\frac{\beta}{V_0P_S}\left(C_{df}D_n\pi x_{f0}\sqrt{\frac{2P_S}{\rho}}\cdot\frac{1}{2\sqrt{\bar{P}_0-\bar{P}_{e0}}}\right)$$

Differential equation for pressure in drain chamber

$$\frac{d}{dt}(\Delta\bar{P}_e)=-K_e\Delta\bar{P}_e+K_f(\Delta\bar{P}_{n1}+\Delta\bar{P}_{n2}) \tag{30}$$

Here,

$$K_e=\frac{\beta}{V_{d0}P_S}\left\{2C_{df}D_n\pi x_{f0}\sqrt{\frac{2P_S}{\rho}}\left(\frac{1}{2\sqrt{\bar{P}_0-\bar{P}_{e0}}}\right) + C_{dd}A_d\sqrt{\frac{2P_S}{\rho}}\cdot\left(\frac{1}{2\bar{P}_e}\right)\right\}$$

$$K_f=\frac{\beta}{V_dP_S}\left(C_{df}D_n\pi x_{f0}\sqrt{\frac{2P_S}{\rho}}\cdot\frac{1}{2\sqrt{\bar{P}_0-\bar{P}_{e0}}}\right)$$

3.1.2 Derivation of transfer funtion

When Laplace transform is executed toward hydraulic servovalve's linearization model obtained in the above, following transfer function expression is derived;

$$(J_as^2+B_as+K_a)\Theta = K_1(\Delta\bar{P}_{n1}(s) - \Delta\bar{P}_{n2}(s))+K_m\bar{I}+K_2\bar{X}_v \tag{31}$$

$$(M_vs^2+B_vs+K_v)X_v = K_3(\Delta\bar{P}_{n1}(s) - \Delta\bar{P}_{n2}(s))+K_4\bar{\Theta} \tag{32}$$

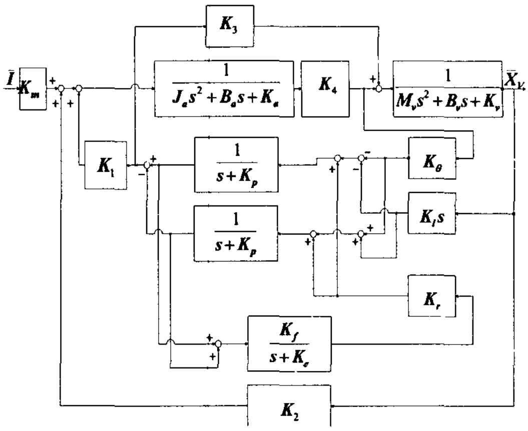

Fig. 6 Block diagram of the electro hydraulic-servo valve.

$$(s+K_p)\Delta\bar{P}_{n1}(s) = -K_\theta\bar{\Theta}-K_ls\bar{X}_v + K_r\Delta\bar{P}_e(s) \tag{33}$$

$$(s+K_p)\Delta\bar{P}_{n2}(s) = K_\theta\bar{\Theta}+K_ls\bar{X}_v + K_r\Delta\bar{P}_e(s) \tag{34}$$

$$(s+K_e)\Delta\bar{P}_e(s) = K_f(\Delta\bar{P}_{n1}(s) + \Delta\bar{P}_{n2}(s)) \tag{35}$$

The spool disposition transfer function and block diagram when inputting electric current, is described in Eq. 36 and Fig. 6 respectively.

$$\frac{\bar{X}_v(s)}{\bar{I}(s)} = \frac{N(s)}{D(s)} \tag{36}$$

Here,

$$N(s)=K_m(s+K_p)\{K_4(s+K_p)-2K_3K_\theta\}$$

$$D(s)=[\{(J_as^2+B_as+K_a)(s+K_p)+2K_lK_\theta\} \times\{(M_vs^2+B_vs+K_v)(s+K_p)+2K_3K_ls\} +\{2K_1K_ls-K_2(s+K_p)\}\{K_4(s+K_p) -2K_3K_\theta\}]$$

3.2. Sensitivity analysis for design parameters

This thesis selected the main design parameter that should be considered when designing

Table 1 Principal design parameters

Index	Symbol	Description
1	K_t	Torque motor gain
2	K_w	Feedback spring stiffness
3	K_f	Flexture tube stiffness
4	D_o	Fixed orifice diameter
5	D_n	Nozzle diameter
6	D	Spool diameter
7	D_d	Drain orifice diameter
8	X_{f0}	Nozzle-flapper initial gap
9	J_f	Flapper rotational inertia
10	B_f	Flapper effective damping coefficient
11	M_s	Spool mass
12	B_s	Spool effective damping coefficient
13	β	Oil effective bulk modulus
14	γ	Flapper length
15	b	Feedback spring length

hydraulic servovalve and examined the system's frequency response characteristics changes shown according to changes of each design parameter. Then, it was aimed to extract factors giving major effects on frequency response characteristics and make use of them as design information. The parameter of this thesis is shown in Table 1.

Figure 7 is bode plot concerning frequency response characteristics of standard servovalve, and represents amplitude ratio and phase difference according to frequency transform.

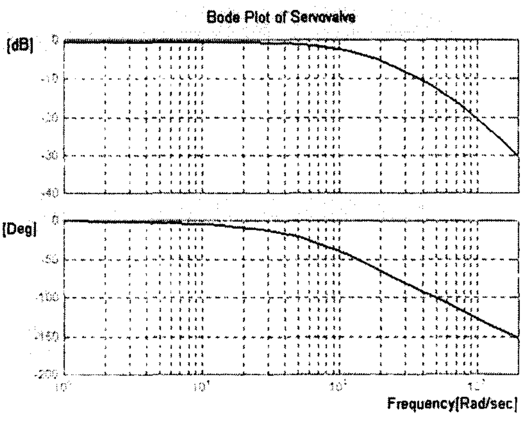

Fig. 7 Bode plot of servo valve.

3.2.1 Definition of parameter sensitivity for frequency response characteristics

The sensitivity function for finding out parameter representing governing influences upon frequency response characteristics of hydraulic servovalve through an interpretive AM (access method) is defined like Eqs. 37 and 38.

Sensitivity for amplitude ratio

$$S_i = \frac{\Delta |G_i(j\omega)|}{|G(j\omega)|} \cdot \frac{p_i}{\Delta p_i} \quad (i=1,2,\ldots,15) \quad (37)$$

Here,

$$\Delta G(j\omega) = |G(j\omega)|_{p_i=\bar{p}_i+\Delta p_i} - |G(j\omega)|_{p_i=\bar{p}_i}$$

$$\Delta p_i = 0.01\bar{p}_i$$

Sensitivity for phase difference

$$S_i = \frac{\Delta(\angle G_i(j\omega))}{\angle G(j\omega)} \cdot \frac{p_i}{\Delta p_i} \quad (i=1,2,\ldots,15) \quad (38)$$

Here,

$$\Delta(\angle G(j\omega)) = \angle G(j\omega)_{p_i=\bar{p}_i+p_i} - \angle G(j\omega)_{p_i=\bar{p}_i}$$

$$\Delta p_i = 0.01\bar{p}_i$$

3.2.2 Review for parameter sensitivity analysis

Figures 8 and 9 show sensitivity analysis results on torque motor gain, flexure tube stiffness coefficient, and feedback spring stiffness coefficient. The sensitivity ratio to torque motor gain ratio shows regular characteristics regardless of frequency, which, in particular, doesn't have effects on phase difference of the system. In case of flexure tube stiffness coefficient, particularly, in case that parameter values rise in the low frequency range, a phase lag effect is shown. A rise of feedback spring constant causes a fall of gain ratio, which effect is shown in the range of low frequency in particular.

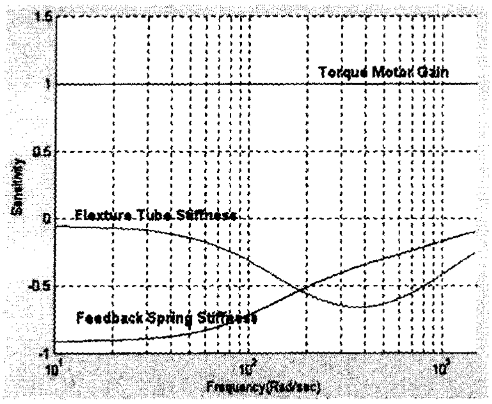

Fig. 8 Amplitude ratio (i=1, 2, 3).

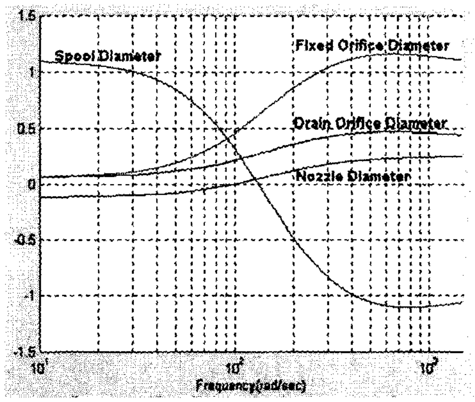

Fig. 10 Amplitude ratio (i=4, 5, 6, 7).

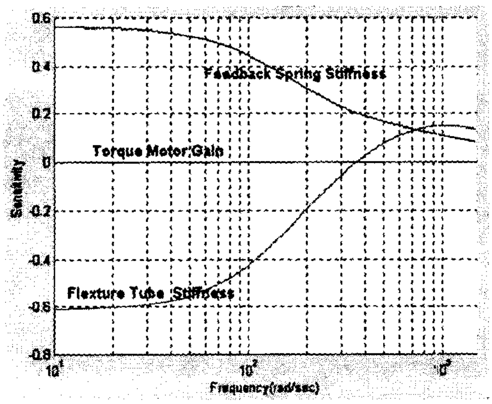

Fig. 9 Phase difference (i=1, 2, 3).

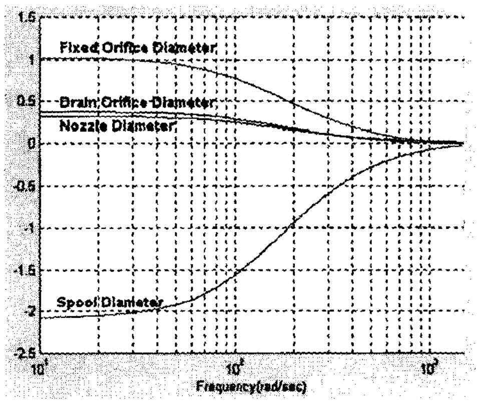

Fig. 11 Phase difference (i=4, 5, 6, 7).

Figures 10 and 11 show sensitivity analysis results on hydraulic servovalve's spool diameter, fixed orifice diameter, drain orifice diameter, and nozzle diameter. In case of fixed orifice diameter and drain orifice diameter, gain ratio increases, phase difference also shows a character of phase lead. But gain ratio shows governing effects in the range of high frequency and phase difference shows governing effects in the area of low frequency. Sensitivity characteristics of spool diameter and nozzle diameter are different in ranges of frequency. In particular, effects of spool diameter are comparatively bigger, characteristics of the system change as follows; gain ratio rises according to value-rise and falls in the area of high frequency. Nozzle shows opposite characters, but in case of nozzle, its SG (specific gravity) is lower when compared with spool diameter. Sensitivity toward phase difference between two parameters is shown in the range of low frequency.

Figures 12 and 13 represent sensitivity analysis results on clearance between flapper and nozzle at null [m]. In particular, sensitivity toward gain ratio is dominant in the area of high frequency and sensitivity toward phase difference is dominant in the area of low frequency. But when considering sensitivity of parameters stated in the above, system frequency response characters are comparatively insensitive toward parameter changes.

Figures 14, 15, 16, and 17 show influences and influence results of inertia · viscosity related

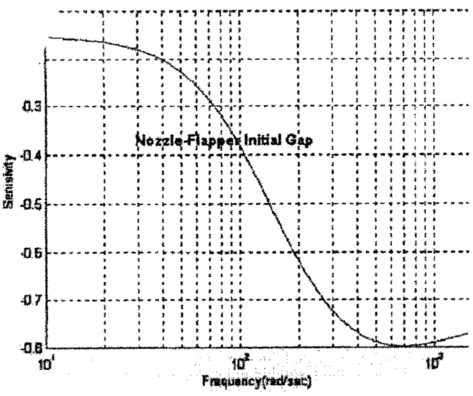

Fig. 12 Amplitude ratio (i=8).

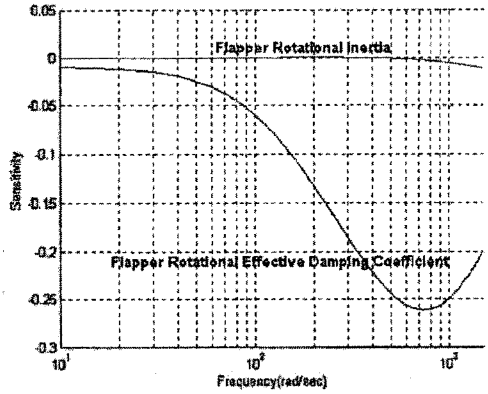

Fig. 15 Phase difference (i=9, 10).

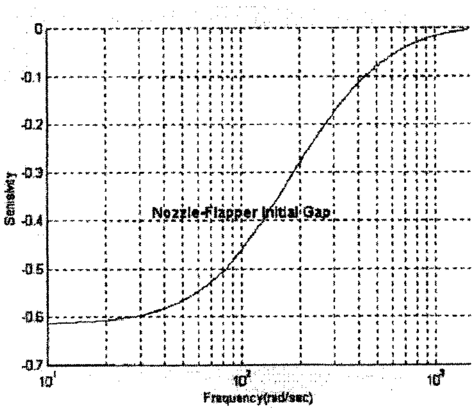

Fig. 13 Phase difference.

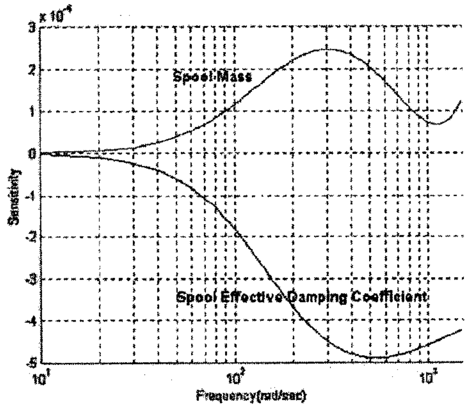

Fig. 16 Amplitude ratio (i=11, 12).

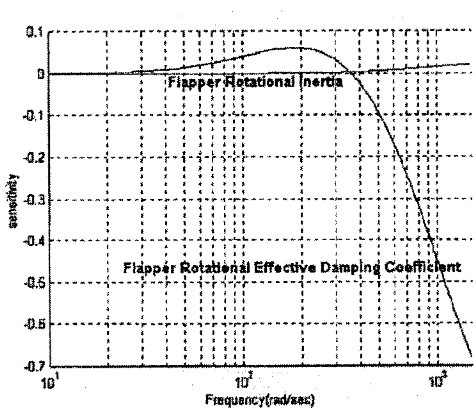

Fig. 14 Amplitude ratio (i=9, 10).

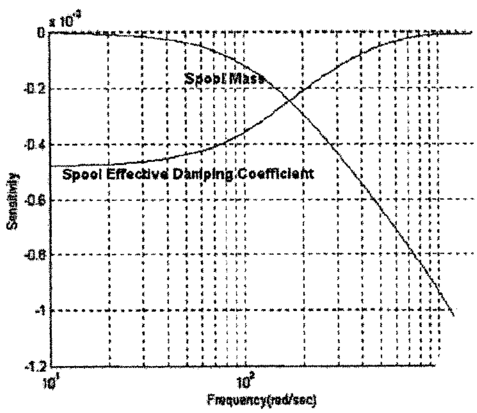

Fig. 17 Phase difference (i=11,

parameter changes upon changes of system frequency response characteristics, in movement ··ation of flapper and spool. As shown in

results of interpretation, spool's m and quantity) changes and viscosi' changes had no effects on chang characteristics, which is shown quantitatively. The rotational inertia of flapper is identical, but changes of effective viscous coefficient in flapper-nozzle part, which are caused by fluid, had comparatively bigger effects on other dynamic parameters in the area of high frequency over system natural frequency.

4. Conclusions

This thesis examined movement characteristics of hydraulic servovalve and executed modeling in each main part of valve through dynamic characteristics interpretation of flapper-nozzle and feedback spring and flow interpretation according to spool disposition, in flapper-nozzle type 2 step power-feedback type flow control electrohydraulic servovalve.

Also, sensitivity toward frequency response characteristics was interpreted. This thesis suggested the 6th system's transfer function model from the Linearization equation, defined sensitivity function toward each parameter's changes in servovalve, and quantitatively derived influences of each parameter upon the whole system's dynamic characteristics, then compared them. This thesis made a standard to effectively improve dynamic characteristics of servovalve.

Acknowledgements

This work was partially supported by the grants from the Brain Korea 21 project, NURI project and Korea Sea Grant Program by Ministry of Marine Affairs & Fisheries and through assistance of Tongmyung Heavy Industries Co. Ltd., in appreciation of their cooperation.

References

1. Martin, D. J. and Burrows, C. R., Dec. 1976, The dynamic characteristics of a electro-hydraulic servovalve, ASME Journal of Dynamic Systems, Measurement and Control, pp. 395-406.
2. Merritt, H. E., 1967, Hydraulic control systems, John Wiley Inc.
3. Feng, T. Y., Sept. 1959, Static and dynamic control characteristics of flapper-nozzle valves, Trans. ASME Journal of Basic Engineering, pp. 275-284.
4. Lin, S. J. and Akers, A., 1989, A dynamic model of the flapper-nozzle component of an electrohydraulic servovalve, ASME Journal of Dynamic Systems, Measurement and Control, Vol. 111, pp. 105-111.
5. Lin, S. J. and Akers, A., 1991, Dynamic analysis of a flapper-nozzle valve, ASME Journal of Dynamic Systems, Measurement and Control, Vol. 113, pp. 163-167.
6. Walters, R., 1967, hydraulic and electro-hydraulic servo systems, Cleveland, CRC Press.
7. Watton, J., 1989, Fluid power systems, Prentice-Hall.
8. Kim, G. D., 1998 A study on the design and the dynamic characteristics of electro-hydraulic flow control servo valve, M.S thesis, Changwon National University.
9. MOOG Technical Bulletine, MOOG Inc.
10. Seo, J. S., 2002, The numerical modeling and the dynamic characteristics of High Respone flow control servo valve, Proceedings of the KSME Autumn Annual Meeting, pp. 7-15.